# Article Title Page

**Adaptive mesh refinement for finite element analysis of the free vibration disturbance of cylindrical shells due to circumferential micro-crack damage**

**Author Details:**

**Yongliang Wang**

School of Mechanics and Civil Engineering, China University of Mining and Technology, Beijing 100083, China; State Key Laboratory of Coal Resources and Safe Mining, China University of Mining and Technology, Beijing 100083, China

**Jiansong Hu**

School of Mechanics and Civil Engineering, China University of Mining and Technology, Beijing 100083, China

**David Kennedy**

School of Engineering, Cardiff University, Queen's Buildings, The Parade, Cardiff, CF24 3AA, UK

**Jianhui Wang**

School of Mechanics and Civil Engineering, China University of Mining and Technology, Beijing 100083, China

**Jiali Wu**

School of Mechanics and Civil Engineering, China University of Mining and Technology, Beijing 100083, China

Corresponding author: Yongliang Wang, wangyl@cumtb.edu.cn

*NOTE: affiliations should appear as the following: Department (if applicable); Institution; City; State (US only); Country.*
*No further information or detail should be included*

## ABSTRACT

### Purpose

Moderately thick circular cylindrical shells are widely used as supporting structures or storage cavities in structural engineering, rock engineering, and aerospace engineering. In practical engineering, shells often work with micro-cracks or defects. The existence of micro-crack damage may result in the disturbance of dynamic behaviours and even induce accidental dynamic disasters. The free vibration frequency and mode are important parameters for the dynamic performance and damage identification analysis. In particular, stiffness weakening of the local damage region leads to significant changes in the vibration mode, which makes it difficult for the mesh generated in the conventional finite element method to capture a high-precision solution of the local oscillation.

### Design/methodology/approach

In response to the above problems, this study developed an adaptive finite element method and a crack damage characterisation method for moderately thick circular cylindrical shells. By introducing the inverse power iteration method, error estimation, and mesh subdivision refinement technique for the analysis of finite element eigenvalue problems, an adaptive computation scheme was constructed for the free vibration problem of moderately thick circular cylindrical shells with circumferential crack damage.

### Findings

Based on typical numerical examples, the established adaptive finite element solution for the free vibration of moderately thick circular cylindrical shells demonstrated its suitability for solving the high-precision free vibration frequency and mode of cylindrical shell structures. The any order frequency and mode shape of cracked cylindrical shells under the conditions of different ring wave numbers, crack locations, crack depths, and multiple cracks were successfully solved. The influences of the location, depth, and number of cracks on the disturbance of dynamic behaviours were analysed.

### Originality/value

This study can be used as a reference for the adaptive finite element solution of free vibration of moderately thick circular cylindrical shells with cracks and lays the foundation for further development of a high-performance computation method

suitable for the dynamic disturbance and damage identification analysis of general cracked structures.

**KEYWORDS:** moderately thick circular cylindrical shell; crack damage; free vibration; vibration disturbance; finite element method; mesh refinement

**ARTICLE CLASSIFICATION:** Research paper

## 1. Introduction

The dynamic analysis of structures and elastomers is an important basis for the study of structural earthquake resistance and rock-induced earthquakes (Ide *et al*., 2016; Chestler *et al*., 2017). As a supporting structure or storage cavity, the cylindrical shell is widely used in structural engineering, rock engineering, and aerospace engineering, and studying the dynamic characteristics of the structure, such as vibration, instability, and buckling, is of great significance for studying and judging its failure behaviour (Dey *et al*., 2017). Nondestructive experimental methods for computing the buckling load of imperfection-sensitive thin-walled structures are one of the most important techniques for the validation of new structures and numerical models of large-scale aerospace structures (Arbelo *et al*., 2014). In the study of structural dynamics, natural frequency and vibration mode are used as mechanical response parameters to analyse dynamic characteristics (Kang *et al*., 2003; Sivadas *et al*., 1994), and have become key research areas. These frequency and vibration modes are also regarded as eigenvalues and eigenfunctions of mathematical eigenvalue problems, which are solved. The circular cylindrical shell has, among other characteristics, clear force, symmetrical structure, and relatively simple manufacturing process (Qu *et al*., 2013). Therefore, the free vibration of a cylindrical shell has been of interest to many researchers (Weingarten, 2012). Consequently, an accurate analysis of the free vibration of circular cylindrical shells is highly valued in practice and research. At present, the traditional thin shell theory is often used to study shell problems. Based on the Kirchhoff–Love assumption (Love, 2013) and ignoring the transverse shear deformation, the theory introduces some errors to a shell structure with small shear stiffness (that is, prone to significant transverse shear deformation). In addition, it underestimates deflections and overestimates the frequencies (Hosseini-Hashemi *et al*., 2011). As many applications of toroidal shells are moderately thick or thick, it is imperative and desirable to establish effective theories appropriate for their analysis (Wang *et al*., 2011). In addition, the increased wall thickness of plate and shell structures in practical engineering is often beyond the application range of the thin-walled theory, and the

influence of transverse shear deformation should also be considered. This study introduced a moderately thick circular cylindrical shell. Compared with the thin shell free vibration theory, the moderately thick shell free vibration theory considers the influence of transverse shear deformation and moment of inertia, which makes the solution more reliable.

Initial defects and factors such as high strength work and long-term use can damage the circular cylindrical shell structure, and cracks are one of the most common defects in most structures. Regarding the power characteristics of the structure, the presence of cracks reduces the original frequency and pushes the resonance band, causing structural vibration and stress strain aggravation, which increases the length of cracks. Cracks in a structural element in the form of initial defects within the material, or caused by fatigue or stress concentration, certainly impact the structural integrity (Dong *et al*., 2012). This creates a vicious circle that affects the reliability of the structure and directly threatens its safety. It is necessary to study the dynamic characteristics of a cracked structure, particularly the characteristics of free vibration. Therefore, in structural design and engineering applications it is important to study the mechanical properties of cracks and to clarify the ultimate bearing capacity of structures containing cracks. Cracks are one of the most common defects in engineering structures; their existence inevitably leads to a decrease in the ultimate bearing capacity of structures or components, and structural fractures will lead to significant economic losses (Wei *et al*., 2014).

In the study of the vibration of cracked cylindrical shells, it is necessary to analyse the influence of different crack positions, sizes, and numbers. Compared with functionally graded beams with a single crack, beams with two or more cracks have lower frequency values (Aydin, 2013). To investigate the influences of the crack depth and position of each crack on the vibration mode and natural frequencies of a simply supported beam, the equation of motion was derived using Hamilton's principle and analysed using a numerical method (Yoon *et al*., 2007). To learn about the effects of the position and depth of each crack on the natural frequency of a simply supported double-cracked beam, a free vibration analysis of cylindrical shells with

circumferential stiffeners was also conducted (Jafari *et al*., 2006). To understand the free vibrations of circular cylindrical shells of piecewise constant thickness when circular cracks of constant length are controlled, an approximate method for the vibration analysis of stepped shells accounting for the influence of cracks located at the re-entrant corners of steps was presented (Jaan *et al*., 2010). To analyse the coupled vibration feature of a fluid-filled cylindrical shell with a circumferential surface crack, the effects of crack depth, crack location, and boundary conditions on the cylindrical shell's modal power flow index were also analysed (Jin *et al*., 2018). To determine the effects of various geometric properties on the vibration and damping factors of circular cylindrical shells, an improved shell theory with shear deformation and rotatory inertia was used (Sivadas *et al*., 1994). To implement a straightforward computer simulation under different shell theories and boundary conditions, the Rayleigh–Ritz method was used to analyse the free vibration of a circular cylindrical shell on a dynamic model (Lee *et al.*， 2015). To obtain solutions for the problem of free non-axisymmetric vibration of stepped circular cylindrical shells with cracks, the influence of circular cracks with constant depth on the vibration of the shell was prescribed with the aid of a matrix of local flexibility (Roots, 2014). Most research in the area of vibration analysis and crack detection of cracked structures has focused on beams (Yin *et al*., 2013). To determine the effect of the development and propagation of cracks on cracked cylindrical shells with various parameters, the effect of a complete penetration non-propagating macro-crack damage on natural vibration frequencies and mode shapes was examined (Dehghani *et al*., 2008). However, there is a lack of research on the influence of vibration on the location, depth, number, and distribution of damage with annular cracks in cylindrical shells. If these problems are not clear, it is difficult to evaluate the vibration disturbance behaviour of cylindrical shells according to crack damage, and it is more difficult to further identify crack damage information according to vibration.

Some theoretical methods, experiments, and numerical computations have been developed to study the free vibration of medium-thick cylindrical shells with cracks. To identify the crack location and depth, an approach was presented to analyse the

wave and vibrational power flow characteristics in cracked cylindrical shell structures (Zhu *et al*., 2007). To conduct a modal analysis of the vibration response of a cracked fluid-filled cylindrical shell, a high-order partial differential equation of thin shell motion was derived (Zheng, 2021). In the development of a research on the free vibration of medium-thick cylindrical shells, the dynamic stiffness method was introduced in the study of moderately thick circular cylindrical shells (Chen and Ye, 2016; Chen and Zhang, 2006). The free vibration of cylindrical shells under homogeneous boundary conditions was studied based on the theory of Flugge (1973) and elastic thin shells (Wang and Huang, 2017). To study the effect of cracks on the natural frequencies and mode shapes of cracked beams, an exact approach for free vibration analysis of a non-uniform beam with an arbitrary number of cracks and concentrated masses was proposed (Li, 2001). To study the influence of a change in shell thickness on the distribution of its natural frequencies, the spline collocation method for finding the frequencies of free vibrations of circular closed cylindrical shells of variable thickness in the circumferential direction was introduced (Grigorenko *et al*., 2010). A holographic interferometry technique was used to determine the frequencies of the free vibrations of isotropic circular cylindrical shells (Grigorenko *et al*., 2011). To improve the computational efficiency and accuracy, a general framework was proposed to analyse the vibration of circular cylindrical shells, both in the case of linear and nonlinear vibrations (Pellicano, 2007). At present, there is a lack of a reliable and high-precision analysis of the frequency and mode of vibration of the disturbed mode of cylindrical shells with crack damage.

For the numerical models and analysis of eigensolutions, the finite element method is widely used to solve the free vibration of moderately thick circular cylindrical shells with complex structures and boundary conditions. The adaptive algorithm for the finite element method has become an important method for optimising the mesh and improving the solution accuracy (Zienkiewicz and Zhu, 1992; Zienkiewicz, 2006; Bespalov *et al.,* 2017; Wang, 2021). It mainly includes the *p*-adaptive method (Arthurs *et al*., 2013) for improving the element order, *h*-adaptive method for increasing the mesh density (Wang, 2020b), and *hp*-adaptive method

(Gomez-Revuelto *et al*., 2012), which combines the above two methods. Through high-performance computations, an adaptive analysis of the finite element method makes it possible to reliably solve challenging issues such as eigenvalue problems, damage, and fracture (Wang, 2020a; Wang *et al*., 2018a; Wang *et al*., 2019). An error analysis of local imperfections based on numerical solutions (Babuska and Rheinboldt, 1978; Babuska and Rheinboldt, 1979) was proposed, and the energy norm measurement method was used to compute the elements with the largest local imperfections. Oden and Ainsworth (Ainsworth and Oden, 1992; Ainsworth and Oden, 1993) also made significant contributions to the analysis of residual errors. In the study of the free vibration of cylindrical shells, the adaptive finite element method can effectively provide higher precision solutions for the analysis. To predict crack-induced natural frequency changes, an accurate and efficient method for analysing the vibration characteristics of cylindrical shells with a part-through crack was proposed (Yin *et al*., 2013). The non-uniform mesh in a high-performance adaptive analysis process is a crucial factor for efficient computation, in which the minimum number of elements and optimised distribution of nodes are used to reduce the solution errors quickly and derive high-precision solutions (Arndt *et al*., 2010; Schillinger *et al*., 2011; Bao *et al*., 2012). The displacement superconvergent patch recovery method of finite elements (Wiberg *et al.*, 1999a; Wiberg *et al.*, 1999b; Wang *et al*., 2018b; Wang, 2020b) was proposed for establishing the mesh refinement procedure for computing high-precision modal shapes. The adaptive finite element method was used to analyse the free vibration of beams with multiple cracks and damage detection (Wang *et al*., 2018b). This study extends this method to the vibration disturbance problem of moderately thick circular cylindrical shells with crack damage.

The remainder of this paper is organised as follows. In Section 2, we present the differential equations describing the free vibration of moderately thick circular cylindrical shell. The damage characterisation method for circumferential cracks in a circular cylindrical shell is introduced in Section 3. In Sections 4 and 5, the key techniques used in the adaptive analysis procedure, such as error estimation for eigenfunctions and *h*-version mesh refinement, are presented. Representative numerical examples are presented in Section 6 to demonstrate the performance of the proposed method and algorithm. Finally, the main conclusions are summarised in Section 7.

## 2. Differential equations describing the free vibration of moderately thick circular cylindrical shell

The geometrical model, coordinate systems, and parameters describing the moderately thick circular cylindrical shell with circumferential cracks investigated in this study are shown in Figure 1. The rotation axis is denoted by $ox$. The local coordinate system at point $A$ on the mid-plane is defined by $\overline{\alpha}\,\overline{\beta}\,\overline{\gamma}$, where $\overline{\alpha}$ points along the tangential direction of the meridian (the direction of the shell axis), $\overline{\beta}$ points along the tangential direction of the weft circle, and $\overline{\gamma}$ points along the normal direction. There is a circumferential surface micro-crack in the cylindrical shell, which is located at length $s$ along the rotation axis, and the depth of the crack is along the thickness of the shell. The five independent displacements of the shell are the linear displacements $u$, $v$, and $w$ along the $\overline{\alpha}$, $\overline{\beta}$, and $\overline{\gamma}$ directions, respectively, and the angular displacements $\phi$ and $\psi$ defined around the $\overline{\gamma}$ and $\overline{\beta}$ directions, respectively. The radius of the middle shell surface is $r$, the section thickness is $h$, the shear stiffness correction factor of the section is $\kappa$, the moment of inertia is $J$, the length is $l$, the elastic modulus of the material is $E$, the shear modulus is $G$, Poisson's ratio is $\mu$, and density is $\rho$.

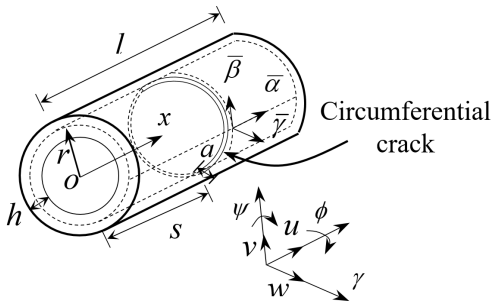


**Figure 1.** Geometrical model, coordinate systems, and symbols describing a moderately thick circular cylindrical shell with circumferential crack.

The governing differential equations of the free vibration of the shell are

$$\begin{aligned}&(1/2)K[(1-\mu)n^2u/r^2-2u''-(1+\mu)nv'/r-2\mu w'/r]\\&\quad=\omega^2\rho hu\end{aligned}, \tag{1a}$$

$$(1/2)K[(1+\mu)nu'/r+2n^2v/r^2-(1-\mu)(1+h^2/12r^2)v''+2nw/r^2 \\ +(1-\mu)nh^2\phi'/(12r^2)-(1-\mu)h^2\psi''/(12r)] \\ +\bar{\kappa}Gh(v/r^2+nw/r^2-\psi/r)=\omega^2\rho hv \quad (1b)$$

$$K(\mu u'/r+nv/r^2+w/r)+\bar{\kappa}Gh(n^2w/r^2+nv/r^2-n\psi/r-w''-\phi') \\ =\omega^2\rho hw \quad (1c)$$

$$(h^2/24)K[-(1-\mu)nv'/r^2+(1-\mu)n^2\phi/r^2-2\phi''-(1+\mu)n\psi'/r] \\ +\kappa Gh(w'+\phi)=\omega^2\rho J\phi \quad (1d)$$

$$(h^2/24)K[-(1-\mu)v''/r+(1+\mu)n\phi'/r+2n^2\psi/r^2-(1-\mu)\psi''] \\ +\kappa Gh(\psi-v/r-nw/r)=\omega^2\rho J\psi \quad (1e)$$

where the prime mark ($'$) denotes the derivative with respect to the independent variable $x$, $K=Eh/(1-\mu^2)$ is the shell stiffness, $\omega$ is the frequency, and $n$ is the circumferential wave number.

The eigenproblem solved in this study includes determining the eigenvalues $\lambda$ and associated $n_d$ dimensional vector eigenfunctions $\mathbf{u}(x)=(u_1(x),..,u_{n_d}(x))^T=(u,v,w,\phi,\psi)^T$ for the following system of second-order ordinary differential equations (ODEs) (Greenberg, 1991; Kurochkin, 2014):

$$\mathbf{Lu}\equiv\mathbf{Au}''+\mathbf{Bu}'+\mathbf{Cu}=\lambda\mathbf{Ru}, \quad a<x<b, \quad (2)$$

where $\mathbf{L}$ is the differential operator, $\mathbf{A}$, $\mathbf{B}$, $\mathbf{C}$, and $\mathbf{R}$ are continuous $n_d\times n_d$ matrix functions on $(a,b)$, and $n_d$ = 5 is associated with the governing differential equations for the free vibration of the shell, as shown in Equation (1). Structural vibration problems were chosen to illustrate the possible physical interpretations of the equations. The corresponding structural natural frequencies ($\omega=\sqrt{\lambda}$) and modes represent the eigenvalues and vector eigenfunctions, respectively.

## 3. Damage characterisation method for circumferential cracks in circular cylindrical shell

In this study, the damage defect characterisation and rotating spring techniques used to characterise the micro-crack in the beams (Wang, 2018b) are extended to this method

to implement damage characterisation in a cylindrical shell. As shown in Figure 2, the geometric model of the moderately thick circular cylindrical shell embedded a circumferential crack, in which the parameters $\alpha$ and $\beta$ denote the normalised crack depth and location, respectively:

$$\alpha = a/h, \tag{3a}$$

$$\beta = s/l, \tag{3b}$$

where $a$ and $s$ are the absolute crack depth and location, respectively, and $h$ is the height of the shell.

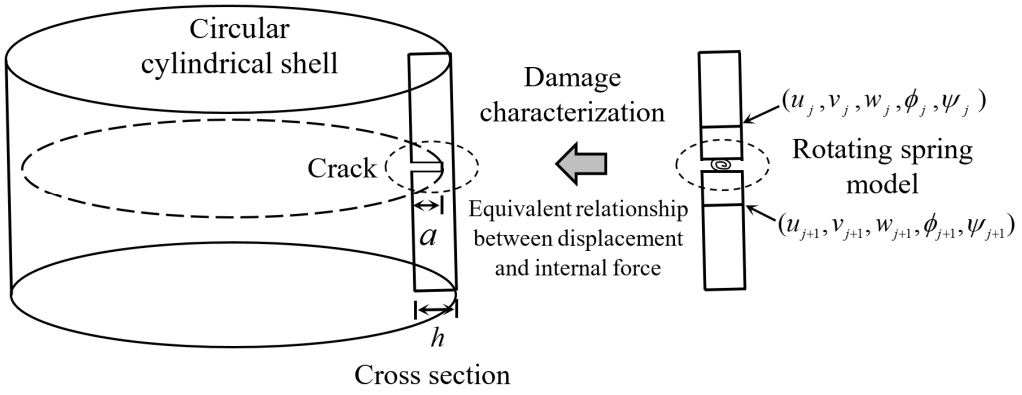


**Figure 2.** Damage characterisation for circumferential crack in circular cylindrical shell.

The local domain around the micro-crack of the shell is shown in Figure 4. In the immediate region surrounding a single crack, the finite element containing the crack has two nodes with the degrees of linear and angular freedoms $(u_j, v_j, w_j, \phi_j, \psi_j)$ and $(u_{j+1}, v_{j+1}, w_{j+1}, \phi_{j+1}, \psi_{j+1})$, where the narrow crack is described with a width $\delta_c$ set at $0.01 \times Tol$, where $Tol$ is the pre-specified error tolerance for both frequencies and modes. Using the weakened properties analogy to reflect the presence of cracks, the shell stiffness and moment of inertia at the crack are reduced as the crack deepens:

$$K_c = Eh(1-\alpha)/(1-\mu^2), \tag{4a}$$

$$J_c = \frac{bh^3(1-\alpha)^3}{12}, \tag{4b}$$

where $EI_c$ and $J_c$ are the shell stiffness and moment of inertia at the crack $c$, respectively, and $b$ is the width of the shell (the value is taken as 1 representing the unit width).

## 4. *h*-version mesh refinement method for eigensolutions of cracked circular cylindrical shell

### *4.1. Finite element solutions*

The Lagrange interpolation formula provides a simple construct for higher-order shape functions that satisfy Equation (2).

$$l_a^p(\xi)=\prod_{\substack{b=1\\ b\neq a}}^{n}\frac{(\xi-\xi_b)}{(\xi_a-\xi_b)}=\frac{(\xi-\xi_1)(\xi-\xi_2)(\cdots)(\xi-\xi_{a-1})(\xi-\xi_{a+1})(\cdots)(\xi-\xi_n)}{(\xi_a-\xi_1)(\xi_a-\xi_2)(\cdots)(\xi_a-\xi_{a-1})(\xi_a-\xi_{a+1})(\cdots)(\xi_a-\xi_n)}. \quad (5)$$

The order of this polynomial is $p = n - 1$. Having chosen the end-node locations, the internal values of $\xi_a$ may be spaced in uniform increments. For one-dimensional elements, we can set (Zienkiewicz *et al*., 2015)

$$N_a(\xi)=l_a^p(\xi) \quad (6)$$

to define the shape functions.

The weak form for the eigenproblems in the system of second-order ODEs, as defined in Equation (2), can be expressed as

$$\int_\Omega \left\{\mathbf{v}'^T\mathbf{A}\mathbf{u}'+\mathbf{v}^T[\mathbf{B}\mathbf{u}'+(\mathbf{C}-\lambda\mathbf{R})\mathbf{u}]\right\}\mathrm{d}x=\mathbf{0}, \quad (7)$$

where $\mathbf{v}$ is a trial function and $\Omega$ is the solution domain. The finite element model uses the conventional degree $m$ of polynomial elements. We let *e* denote a typical element with end-node coordinates $\bar{x}_1$ and $\bar{x}_2$ and with length $h$. We write the trial function on an element of degree $m$ as

$$\mathbf{v}=\sum_{i=1}^{m+1}\mathbf{N}_i\mathbf{v}_i, \quad (8)$$

where $\mathbf{N}_i$ is an $n_d \times n_d$ shape function matrix defined by

$$\mathbf{N}_i=N_i\mathbf{I}, \quad i=1,2,...,m+1, \quad (9)$$

where $\mathbf{I}$ is the $n_d \times n_d$ identity matrix.

Using the conventional finite element method, the element stiffness and mass matrices ($\mathbf{K}^e$ and $\mathbf{M}^e$, respectively) are computed and assembled to form the global stiffness and mass matrices $\mathbf{K}$ and $\mathbf{M}$, respectively. The finite element equation is then derived as an eigenvalue equation in the following matrix form:

$$\mathbf{KD}=\lambda\mathbf{MD}, \quad (10)$$

where $\mathbf{D}$ is the eigenfunction vector, and matrices $\mathbf{K}$ and $\mathbf{M}$ are independent of $\lambda$. Based on the inverse iteration technique (Wang *et al*., 2018b), the eigensolutions of Equation (10) can be derived.

*4.2. Error estimation*

The superconvergent patch recovery displacement method was developed (Wiberg *et al.*, 1999a; Wiberg *et al.*, 1999b; Wang *et al*., 2018b; Wang, 2020b) to acquire the superconvergent displacements of the finite element solutions in static and dynamic problems. The displacements provided by this method can be applied to eigenfunctions. For example, if element *e* is a superconvergent computation element and elements *e*–1 and *e*+1 are its neighbouring elements, all finite element nodes in patched elements *e*–1, *e*, and *e*+1 are selected for the computation process. Further, the superconvergent displacements for element *e* can be computed as

$$\mathbf{u}^*(x) = \sum_{i=1}^{r} \mathbf{N}_i(x)\mathbf{u}_i^h + \sum_{i=1}^{s} \mathbf{N}_i(x)\bar{\mathbf{u}}_i^*, \tag{11}$$

where $r = 2$ is the number of end nodes, $s$ is the number of internal nodes, and $\mathbf{N}_i$ is the shape function matrix. Using high-order shape function interpolation, the polynomial order of the shape function is increased, $r + s > m + 1$. To optimise the superconvergent order $O(h^{2m})$ for displacements at the end nodes, the displacement recovery field can be expressed for the finite element nodes as follows:

$$\bar{u}_i^*(x) = \mathbf{P}\mathbf{a}, \qquad i = 1, .., n_d, \tag{12}$$

where $\mathbf{P}$ is the given function vector and $\mathbf{a}$ can be determined by least-squares fitting for the coincidence of displacements at the end nodes in both the recovery and conventional finite element fields. The superconvergent displacements of the recovery field are used in Equation (11) to obtain the superconvergent solutions of element *e*. We use the following forms for the vector coefficients $\mathbf{P}$ and $\mathbf{a}$:

$$\mathbf{P} = \begin{bmatrix} 1 & x & \ldots & x^p \end{bmatrix}, \ \mathbf{a} = \begin{bmatrix} a_1 & a_2 & \ldots & a_m \end{bmatrix}^T \tag{13}$$

The value of $\mathbf{a}$ was determined from the minimum value of the following functional, so that the product of $\mathbf{P}$ and $\mathbf{a}$, computed using Equation (12), matches the displacement values:

$$\Pi = \sum_{j=1}^{n} \left( u_i^*(x_j) - \mathbf{P}(x_j)\mathbf{a} \right), \qquad i = 1, .., n_d, \tag{14}$$

where $n$ is the node number of all elements patched together.

The least-squares method applied to Equation (14) yields

$$\mathbf{a} = \mathbf{A}^{-1}\mathbf{b}\,, \tag{15}$$

with the coefficient matrices **A** and **b** defined as:

$$\mathbf{A} = \sum_{j=1}^{n} \mathbf{P}(x_j)^T \mathbf{P}(x_j)\,, \quad \mathbf{b} = \sum_{j=1}^{n} \mathbf{P}(x_j)^T u_i^h(x_j)\,, \qquad i = 1, .., n_d\,. \tag{16}$$

After $\mathbf{a}$ is determined, the superconvergent solutions of the displacement of the piecewise elements are obtained from Equation (11). The estimated eigenvalue has a stationary value when all possible functions satisfying the essential boundary conditions are considered. These stationary values are the superconvergent eigenvalues. Furthermore, the superconvergent solutions of the displacements can be used in the Rayleigh quotient (Wilkinson, 1965; Wilkinson and Reinsch, 1971) to estimate the eigenvalue as

$$\lambda^* = \frac{a(\mathbf{u}^*, \mathbf{u}^*)}{b(\mathbf{u}^*, \mathbf{u}^*)}, \tag{17}$$

where $a(\cdot)$ and $b(\cdot)$ are the strain and kinematic energy inner products, respectively. To determine whether the solution for the considered mesh meets the required tolerance condition, the error must satisfy the following condition:

$$\left\|\mathbf{e}^*\right\| \le Tol \cdot \left[\left(\left\|\mathbf{u}^h\right\|^2 + \left\|\mathbf{e}^*\right\|^2\right) \Big/ n_e\right]^{1/2}, \tag{18}$$

where $n_e$ is the number of elements, and $\left\|\mathbf{e}^*\right\|$ is the error in the energy norm, as follows:

$$\left\|\mathbf{e}^*\right\| = \left[a(\mathbf{e}^*, \mathbf{e}^*)\right]^{1/2} = \left[\int_\Omega \mathbf{e}^{*T} \mathbf{L} \mathbf{e}^* \, \mathrm{d}x\right]^{1/2}, \tag{19}$$

where $\mathbf{e}^* = \mathbf{u}^* - \mathbf{u}^h$, and $\Omega$ is the solution domain.

*4.3. Element subdivision and refinement*

Equation (18) can be rewritten as

$$\xi \le 1\,, \tag{20}$$

where

$$\xi = \frac{\left\|\mathbf{e}^*\right\|}{\bar{e}} \quad \text{with} \quad \bar{e} = Tol \cdot \left[\left(\left\|\mathbf{u}^h\right\|^2 + \left\|\mathbf{e}^*\right\|^2\right) \Big/ n_e\right]^{1/2}. \tag{21}$$

If Equation (20) is not satisfied, the corresponding element is subdivided into identical sub-elements by inserting interior nodes through *h*-refinement (Wang *et al*., 2018b; Wang, 2020b). These are computed using

$$h_{\text{new}} = \xi^{-1/m} h_{\text{old}}, \tag{22}$$

where $h_{\text{new}}$ is the length of the sub-element and $h_{\text{old}}$ is the original length of element *e*. The above element subdivision approach was implemented as follows:

$$n_{\text{new}} = \min\left(\left\lfloor \xi^{1/m} \right\rfloor, d\right), \tag{23}$$

where $n_{\text{new}}$ is the number of sub-elements after element subdivision, the symbol $\left\lfloor \cdot \right\rfloor$ denotes the 'floor' operator (i.e., the rounding down to the nearest integer), and $d$ is the limit needed to avoid too many redundant elements. Each element *e* that does not meet the pre-specified error tolerance threshold is uniformly subdivided by the *h*-version mesh refinement.

## 5. Global algorithm and procedure

According to the finite element solution, error estimation, mesh subdivision, and refinement methods for free vibration of cylindrical shells with crack damage introduced above, the adaptive finite element algorithm for free vibration disturbance of moderately thick circular cylindrical shells with circumferential micro-crack damage can be established, as shown in Figure 3. First, the basic parameters including the micro-crack damage, physical parameters, circumferential wave numbers, initial mesh, and error *tolerance* should be provided. The procedure involves the following three basic processes:

(1) **Finite element model:** Based on the circular cylindrical shell with circumferential cracks and damage characterisation method, the conventional finite element computation is performed based on the initial mesh. The finite element solutions ($\omega^h$, $\mathbf{u}^h$) under the current mesh were computed.

(2) **Error estimation:** Based on the error estimation technique, the disturbance modes induced by crack damage can be evaluated. It should be noted that in the vicinity of crack damage, owing to the disturbance of the vibration mode, its

solution may produce significant errors. At the same time, the information on whether the error tolerance of each element is met is marked.

(3) **Mesh refinement:** Element subdivision and optimisation around the local domain of crack damage. For the element whose error estimation does not meet the error tolerance condition, the mesh subdivision refinement method is used to subdivide it and obtain a new finite element mesh before returning to step (1). In the local domain of crack damage, owing to the large error, it may be necessary to introduce more subdivided elements. If all the elements meet the error tolerance condition, no subdivision is necessary, and the computation process is completed. Through the above adaptive process, the optimal mesh and high-precision solution under the current eigenvalue order of the cylindrical shell with crack damage can be obtained when the vibration mode is disturbed, which is especially suitable for cylindrical shells with crack damage when the vibration mode is disturbed.

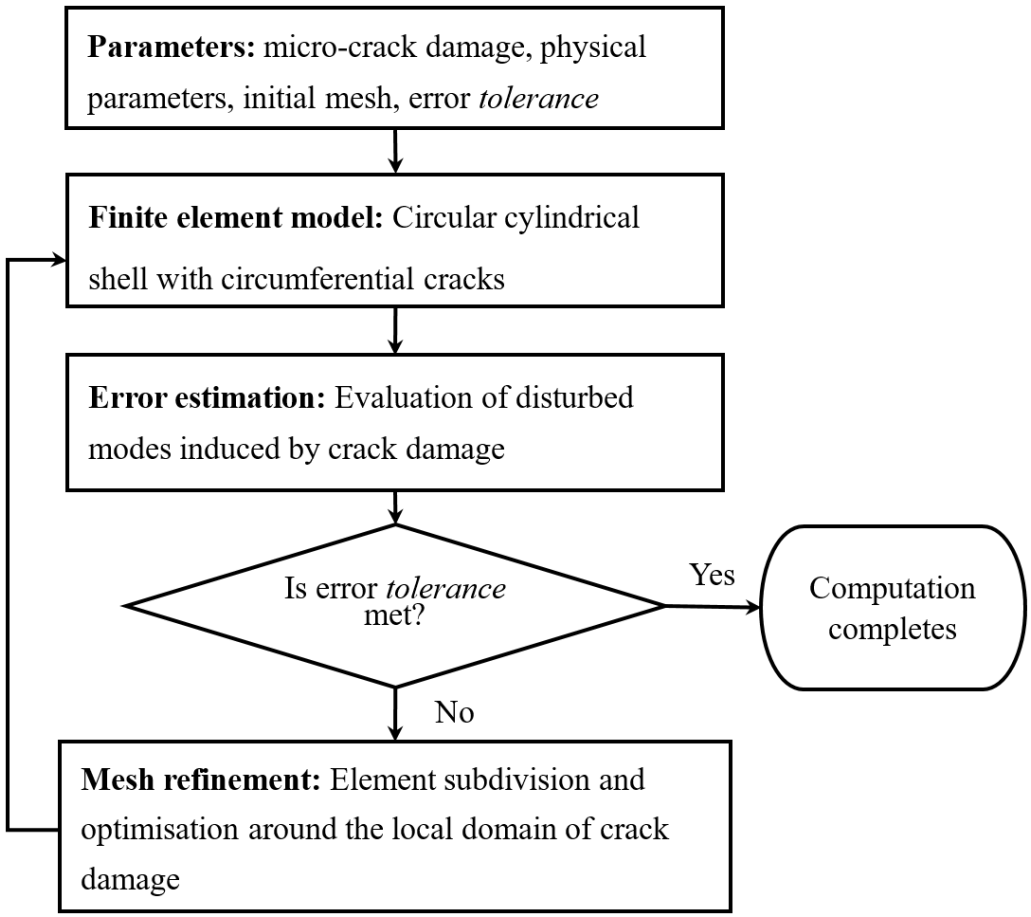


**Figure 3.** Flow chart of the adaptive finite element algorithm and procedure for free vibration disturbance of moderately thick circular cylindrical shells with circumferential micro-crack damage.

## 6. Numerical examples

This section presents some representative numerical examples to demonstrate the performance of the proposed method and algorithm, which were implemented in Fortran 90. The uncracked and cracked damage cases of moderately thick circular cylindrical shells were computed, and the reliability and accuracy of the method described herein were verified. The effects of different crack locations, crack depths, and number of multiple cracks on the free vibration disturbance were analysed. The program was run on a DELL Optiplex 380 Intel (R) Core (TM) 2.93 GHz desktop computer. The degree of element for mesh refinement is $m$ = 3, the initial number of elements used in the computation procedure is $n_e$ = 2, and the stricter pre-specified error tolerance is $Tol = 10^{-6}$. In this study, the mode error introduced in Section 4.2 was used for solution estimation and control. The frequency was computed by the Rayleigh quotient, the error of which needs to be estimated. The relative error $\varepsilon_\omega$ between the exact frequency $\overline{\omega}$ (i.e., the high-precision solutions from other methods) and the computed frequency $\omega^h$ was defined and used to analyse the precision of the solutions:

$$\varepsilon_\omega = \frac{\left|\overline{\omega} - \omega^h\right|}{1 + \left|\overline{\omega}\right|}. \tag{24}$$

### *6.1. Example 1: Benchmarks for free vibration of circular cylindrical shell*

To verify the reliability and accuracy of the method proposed in this study, the free vibration frequency of a circular cylindrical shell without crack damage was computed under the condition of simple support at both ends. The basic geometric and physical parameters of the cylindrical shell are listed in Table 1.

**Table 1.** Geometric and physical parameters of shell in Example 1.

| Parameters | $r$ (mm) | $h$ (mm) | $l$ (mm) | $\mu$ | $\kappa$ | $E$ (GPa) | $\rho$ (kg·m$^{-3}$) |
|---|---|---|---|---|---|---|---|
| Values | 148. 234 | 0. 508 | 298. 2 | 0. 285 | 5/6 | 203. 5 | 7846 |

The method presented in this study was used to solve the first-order ($k$ = 1)

solutions with different circumferential wave numbers $n$ ($n$ = 1–5). The computed frequency results are presented in Table 2. In previous studies (Chen and Ye, 2016; Sivadas and Ganesan, 1994), the dynamic stiffness method and the hybrid finite element method were used to solve the problem, respectively, based on the medium-thick shell theory. It can be observed that the results in this study are in good agreement with those frequency solutions, which verifies the reliability of the method in solving the frequency of each order.

**Table 2.** Computed frequencies $\omega/\mathrm{Hz}$ of shell in Example 1. **Source:** [a] Results from paper Chen and Ye (2016); [b] Results from Sivadas and Ganesan (1994).

| $n$ | $\omega_1^h$ | $\omega_1^h$ [a] | $\omega_1^h$ [b] |
|---|---|---|---|
| 1 | 3270. 74 | 3270. 6 | 3270. 9 |
| 2 | 1862. 12 | 1862. 0 | 1862. 1 |
| 3 | 1101. 83 | 1101. 8 | 1101. 8 |
| 4 | 705. 758 | 705. 9 | 705. 7 |
| 5 | 497. 467 | 497. 5 | 497. 4 |

Figure 4 shows the typical computed vibration modes and the corresponding final meshes on the horizontal $x$-axis for circumferential wave numbers $n$ = 1. The components $(u^h, v^h, w^h)$ and $(\phi^h, \psi^h)$ of the first-order vibration mode with approaching magnitude are shown in Figures 4 (a) and 4 (b), respectively. It should be noted that to facilitate visual display and comparative analysis, the vibration mode results in this study were normalised (make the maximum vibration mode value 1), and the horizontal $x$-axis is also normalised in the vibration mode diagram (the horizontal coordinate axis $x/l$). It can be observed that the vibration mode changes sharply at both ends, and the relatively fine mesh is divided by the adaptive refinement method. The variation of the vibration mode is relatively gentle in the middle domain, and only sparse meshes are optimised and provided. The computation results of the medium-thick cylindrical shell indicate that the adaptive strategy herein is accurate and reliable, and the mesh division is reflected in the error analysis and mesh division described

above.

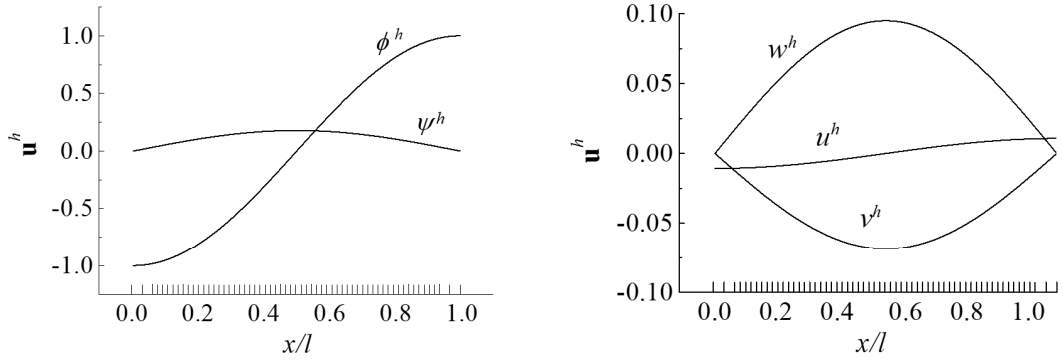


(a) Vibration mode $(\phi^h, \psi^h)$, $k = 1, n = 1$.

(b) Vibration mode $(u^h, v^h, w^h)$, $k = 1, n = 1$.

**Figure 4.** Example 1: computed vibration modes and corresponding final meshes for circumferential wave numbers $n = 1$.

*6.2. Example 2: Verification of frequency solutions of cracked circular cylindrical shell under variable circumferential wave numbers*

The effectiveness of the method proposed in this study for the analysis of cylindrical shells with crack damage was tested. The shell had a crack damage located at $\beta = 0.3$ with a depth $\alpha = 0.6$. The solutions under different frequency orders and circumferential wave numbers were computed and discussed. The geometric and physical parameters of the shell are listed in Table 3.

**Table 3.** Geometric and physical parameters of shell in Example 2.

| Parameters | $r$ (mm) | $h$ (mm) | $l$ (mm) | $\mu$ | $\kappa$ | $E$ (GPa) | $\rho$ (kg·m$^{-3}$) |
|---|---|---|---|---|---|---|---|
| Values | 100 | 2 | 500 | 0.3 | 5/6 | 210 | 7850 |

Using the proposed method, the frequencies and vibration modes of cracked cylindrical shells with different orders $k$ ($k$ = 1–3) and circumferential wave numbers $n$ ($n$ = 1–5) were solved. Table 4 lists the computed frequency solutions under various circumferential wave numbers. To solve the numerical example of the free vibration of a cylindrical shell with damage, the results were obtained using the conventional finite element method and the beam function and Soedel's expression method (Yin and Lam, 2013). For comparative analysis, the relative error between the frequency results of the

proposed method and the frequency result computed in the above study are listed in Table 4, which shows that the error is very small, verifying the effectiveness of the method in this study. At the same time, the results of the final adaptive mesh number $n_e$ for various cases are presented.

**Table 4.** Computed frequencies of cracked circular cylindrical shell under variable circumferential wave numbers in Example 2. **Source:** [a] Results from paper Yin and Lam (2013).

| $k$ | $n$ | Conventional finite element method $\omega^h$ [a] | Beam function and Soedel's expression method $\omega^h$ [a] | $\omega^h$ | Error (%) | $n_e$ |
|---|---|---|---|---|---|---|
| 1 | 3 | 509.10 | 510.54 | 511.47 | 0.18 | 85 |
| 1 | 2 | 665.15 | 652.61 | 658.32 | 0.87 | 93 |
| 1 | 4 | 766.54 | 767.28 | 769.66 | 0.31 | 88 |
| 2 | 4 | 1061.98 | 1066.42 | 1065.26 | 0.11 | 110 |
| 1 | 5 | 1199.35 | 1196.21 | 1197.84 | 0.13 | 91 |
| 2 | 3 | 1229.20 | 1216.05 | 1221.25 | 0.43 | 111 |
| 2 | 5 | 1332.13 | 1335.81 | 1338.43 | 0.20 | 113 |
| 1 | 1 | 1598.83 | 1566.33 | 1548.92 | 1.11 | 106 |
| 3 | 5 | 1678.17 | 1674.43 | 1678.04 | 0.22 | 157 |
| 3 | 4 | 1703.03 | 1696.90 | 1687.82 | 0.53 | 161 |

To illustrate the disturbance of the vibration mode caused by crack damage and the adaptive subdivision and refinement behaviour of the mesh, Figure 5 shows the representative computed vibration modes and corresponding final meshes for a circular wave number $n = 3$. It can be observed that in the domain around the crack damage, the vibration mode changes significantly, and there is a large deformation. In the domain around the crack, the adaptive procedure generates a very dense mesh to capture more refined vibration mode changes.

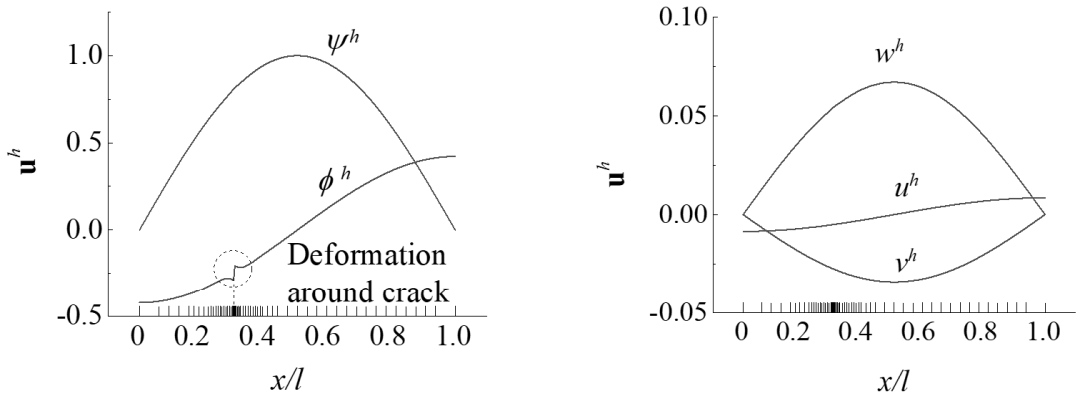


(a) Vibration mode $(\phi^h, \psi^h)$, $k = 1, n = 3$

(b) Vibration mode $(u^h, v^h, w^h)$, $k = 1, n = 3$

**Figure 5.** Example 2: computed vibration modes and corresponding final meshes for circumferential wave number $n = 3$.

To show the disturbance effect of circumferential crack damage and circumferential wave number on spatial vibration modes, Figure 6 shows the spatial morphologies of the vibration modes for a circular wave number $n = 3$. When the circumferential wave number $n$ is 3, there are multiple circumferential waves in the circumferential direction among the five vibration mode components. In the spatial local domain of the circumferential crack damage, the vibration mode fluctuates, which is most obvious in the components shown in Figure 6 (d). A non-uniform mesh was generated on the horizontal axis. According to the above analysis, dense meshes were used in the domain around the crack to solve the five vibration mode components simultaneously.

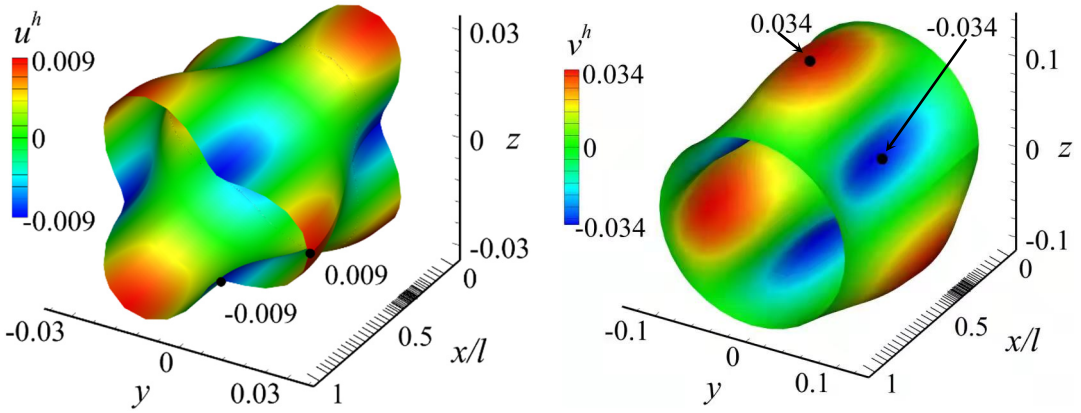


(a) Vibration mode $u^h$, $k = 1, n = 3$

(b) Vibration mode $v^h$, $k = 1, n = 3$

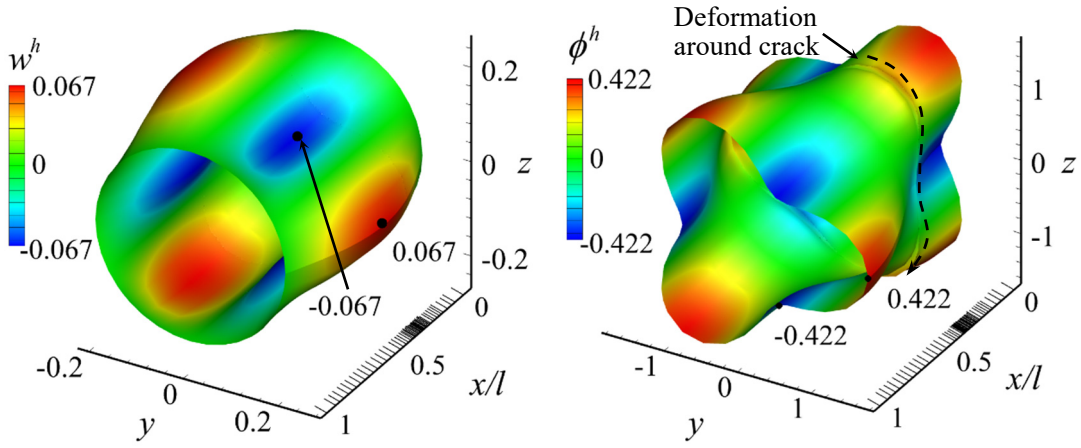


(c) Vibration mode $w^h$, $k = 1$, $n = 3$ (d) Vibration mode $\phi^h$, $k = 1$, $n = 3$

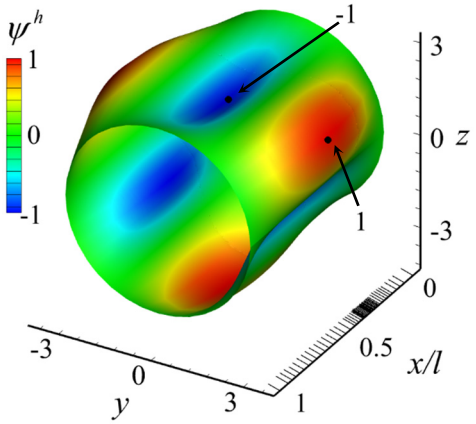


(e) Vibration mode $\psi^h$, $k = 1$, $n = 3$

**Figure 6.** Example 2: Spatial morphologies of vibration modes for circumferential wave number $n = 3$.

To show the influence of different circumferential wave numbers and vibration orders on vibration modes and meshing, Figure 7 shows the representative results of the computed vibration modes and corresponding final meshes for different circular wave numbers. It can be observed from Figures 7 (a)–(d) that with the increase in the wave number of the circumferential vibration mode, the change in the vibration mode along the axial direction is not obvious, but the change in the circumferential vibration mode will show the increase in the wave number. It can be observed from Figures 7 (e)–(f) that with the increase in vibration order, the change in vibration mode along the axial direction will become more complex and more circumferential wave numbers in the vibration modes will appear, which also makes the number of elements in the whole

domain greater than in the first-order vibration mode described in Figures 7 (a)–(d). It can be concluded that the circumferential wave number of rotating shells (such as the circular cylindrical shell in this study) will not have a significant difference with respect to the mesh distribution owing to the symmetry of the vibration mode, but the change in the order of the vibration mode puts forward higher requirements for the number of elements in the whole region. The existence of crack damage makes it necessary to refine the local mesh to capture the disturbance change in the vibration mode.

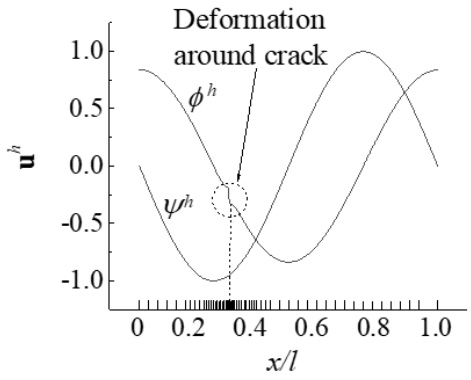


(a) Vibration mode $(\phi^h, \psi^h)$,

$k = 1, n = 4$

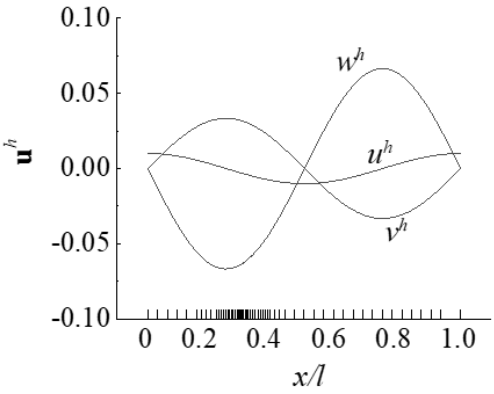


(b) Vibration mode $(u^h, v^h, w^h)$,

$k = 1, n = 4$

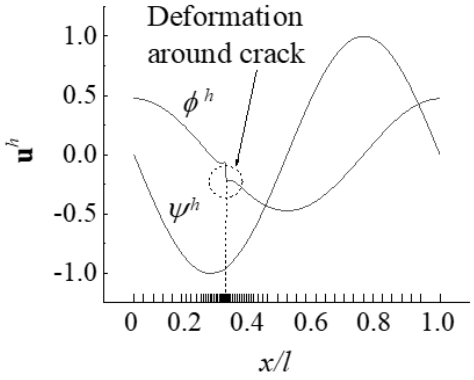


(c) Vibration mode $(\phi^h, \psi^h)$,

$k = 1, n = 5$

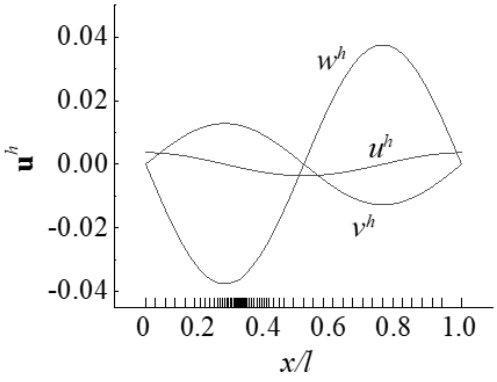


(d) Vibration mode $(u^h, v^h, w^h)$,

$k = 1, n = 5$

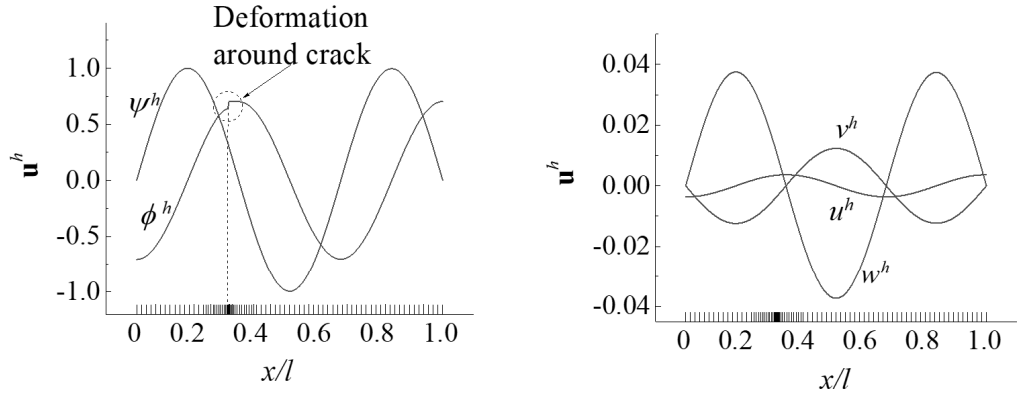


(e) Vibration mode $(\phi^h, \psi^h)$, $k = 2, n = 3$

(f) Vibration mode $(u^h, v^h, w^h)$, $k = 2, n = 3$

**Figure 7.** Example 2: computed vibration modes and corresponding final meshes for different circumferential wave numbers.

*6.3. Example 3: Free vibration disturbance by crack location*

This example discusses the influence of the crack damage location on the vibration disturbance of a cylindrical shell. This example uses the model parameters of Example 2 to change the crack damage location. The crack location $\beta$ was changed from 0.1 to 0.9 with an interval of 0.1. Table 5 lists the computed first-order frequencies for different crack locations. Here, the number of final adaptive elements $n_e$ used is also provided. Figure 8 shows the relationship between the computed frequency and crack location to show the frequency values at different crack damage locations. As can be observed, when the crack damage is at a symmetrical location (such as $\beta$ = 0.2 and 0.8), the same frequency value will appear owing to the structural symmetry of the shell. As indicated in Table 5, the same number of elements was used. At the same time, as shown in Figure 8, when the crack damage occurred at both ends of the cylindrical shell, the stiffness of the shell decreased the most, resulting in a relatively low frequency value. At this time, the stiffness of the shell changed significantly, and more elements were used than when the crack was located in the middle of the shell.

**Table 5.** Computed frequencies under different crack locations in Example 3.

| $\beta$ | $\omega^h$ | $n_e$ |
|---|---|---|
| 0.1 | 10107.48 | 106 |
| 0.2 | 10112. 95 | 112 |
| 0.3 | 10119.72 | 106 |
| 0.4 | 10125.22 | 96 |
| 0.5 | 10127.32 | 88 |
| 0.6 | 10125.22 | 96 |
| 0.7 | 10119.72 | 106 |
| 0.8 | 10112.95 | 112 |
| 0.9 | 10107.48 | 106 |

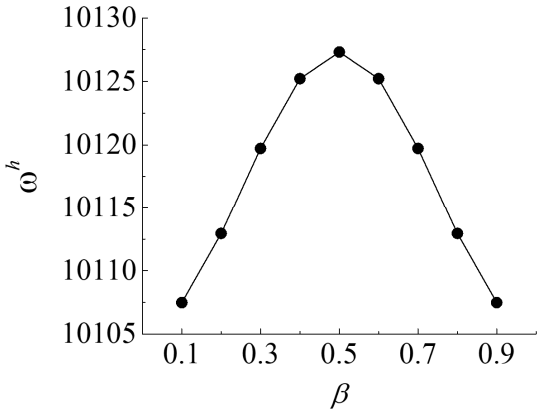


**Figure 8.** Example 2: Relationship between computed frequency and crack location.

Figure 9 shows the computed vibration modes and corresponding final meshes for different crack locations $\beta = 0.1$ and $\beta = 0.5$, respectively. It can be observed that the location of crack damage causes a corresponding disturbance to the vibration mode components, and the local subdivision and refinement domain of the mesh changes with the change in the vibration mode location of the crack damage disturbance. These results demonstrate the effectiveness of the adaptive mesh refinement method on free vibration disturbance by crack location.

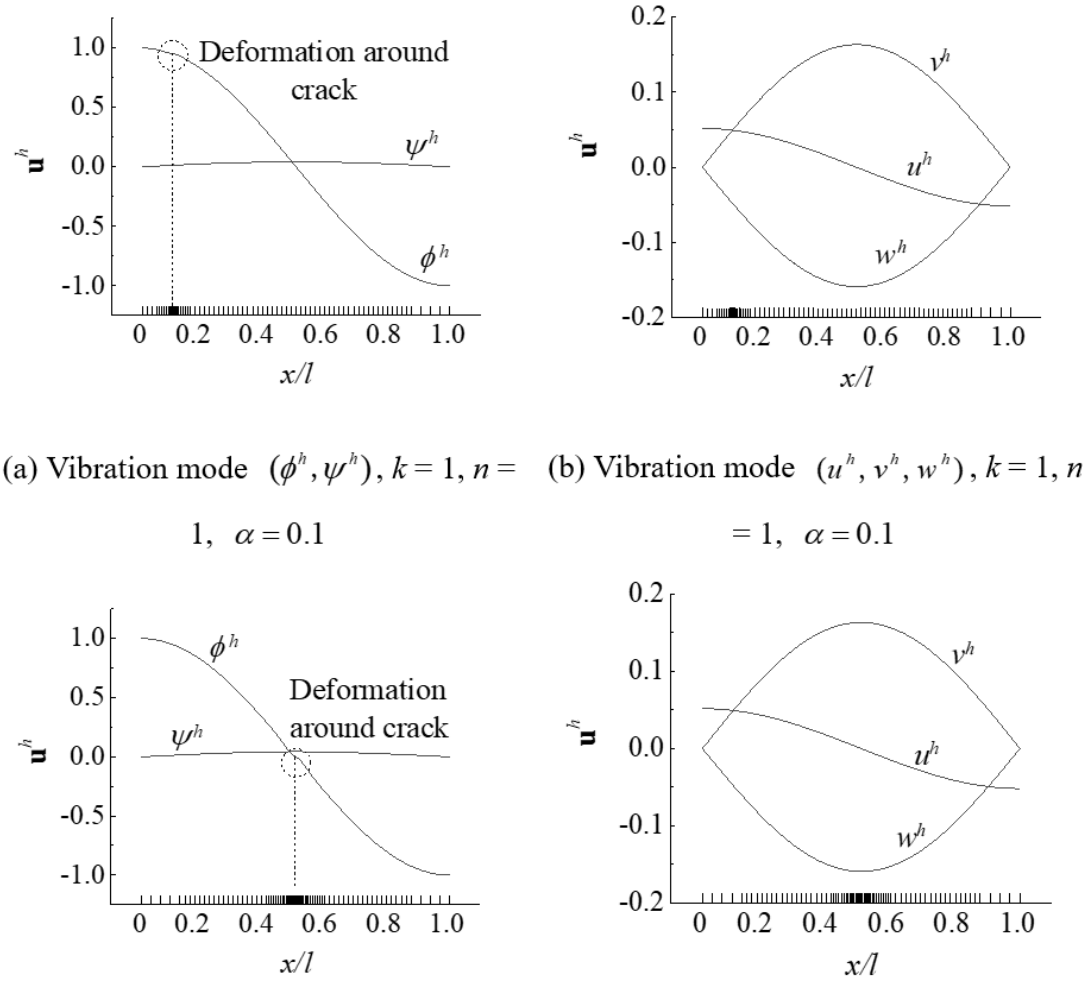


(a) Vibration mode $(\phi^h, \psi^h)$, $k = 1$, $n = 1$, $\alpha = 0.1$

(b) Vibration mode $(u^h, v^h, w^h)$, $k = 1$, $n = 1$, $\alpha = 0.1$

(c) Vibration mode $(\phi^h, \psi^h)$, $k = 1$, $n = 1$, $\alpha = 0.5$

(d) Vibration mode $(u^h, v^h, w^h)$, $k = 1$, $n = 1$, $\alpha = 0.5$

**Figure 9.** Example 3: Computed vibration modes and corresponding final meshes for different crack locations.

*6.4. Example 4: Free vibration disturbance by crack depth*

This example discusses the influence of the crack damage depth on the vibration disturbance of a cylindrical shell. This example uses the model parameters of Example 2 to change the crack damage depth. The crack depth $\alpha$ was changed from 0.2 to 0.6 with an interval of 0.2. Table 6 lists the computed first-order frequencies for different crack depths. Here, the number of final adaptive elements $n_e$ used is also provided. It can be observed that the change in crack damage depth changes the frequency slightly,

but the increase in the degree of crack damage increases the vibration mode disturbance and increases the number of required elements $n_e$ .

**Table 6.** Computed frequencies under different crack depths in Example 4.

| $\alpha$ | $\omega^h$ | $n_e$ |
|---|---|---|
| 0.2 | 10109.38 | 88 |
| 0.4 | 10114.55 | 93 |
| 0.6 | 10119.72 | 106 |

Figure 10 shows the computed vibration modes and corresponding final meshes for different crack depths $\alpha = 0.2$ and $\alpha = 0.4$, respectively. As can be observed, the depth of crack damage causes a corresponding disturbance of the vibration mode component, but the entire shape is basically the same as that in the different crack damage cases. The mesh distribution is basically the same in the entire domain, but it changes in the local domain of the crack damage disturbance mode. The deeper the crack damage is, the more severe the mode damage, and more elements are needed.

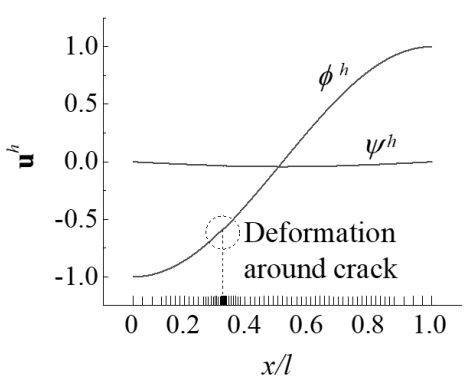


(a) Vibration mode $(\phi^h, \psi^h)$,

$k = 1, n = 1, \ \alpha = 0.2$

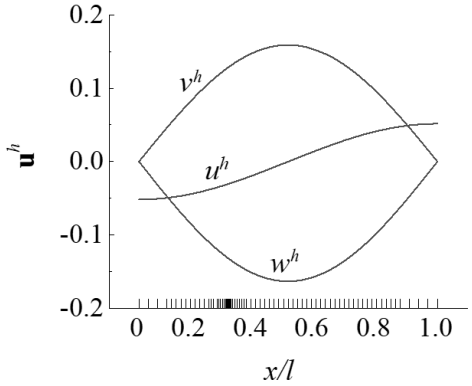


(b) Vibration mode $(u^h, v^h, w^h)$,

$k = 1, n = 1, \ \alpha = 0.2$

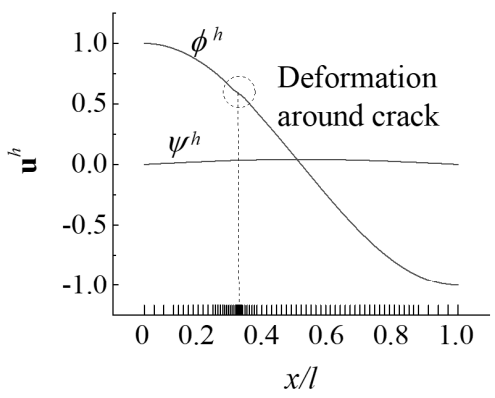


(c) Vibration mode $(\phi^h, \psi^h)$,

$k = 1, n = 1, \ \alpha = 0.4$

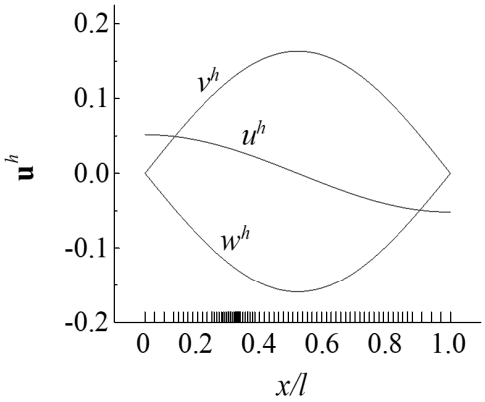


(d) Vibration mode $(u^h, v^h, w^h)$,

$k = 1, n = 1, \ \alpha = 0.4$

**Figure 10.** Example 4: computed vibration modes and corresponding final meshes for different crack depths.

*6.5. Example 5: Free vibration disturbance by number of multiple cracks*

This example discusses the influence of multiple-crack damage on the vibration disturbance of a cylindrical shell. This example uses the model parameters of Example 2 to change the number and location of multiple cracks. The crack location $\beta$ was 0.3, 0.5, 0.7 (for three cracks) and 0.1, 0.3, 0.5, 0.7, 0.9 (for five cracks), respectively. Table 7 lists the computed frequencies for multiple cracks. Here, the number of final adaptive elements $n_e$ used is also provided. As can be observed, the change in the number and location of cracks changes the frequency slightly, but the increase in the number of cracks increases the vibration mode disturbance and increases the number of required elements $n_e$. Compared with 190 elements for the computation of three cracks in the shell, 276 elements are needed for five cracks in the shell.

**Table 7.** Computed frequencies under multiple cracks in Example 5.

| $n_c$ | $\beta$ | $\omega_1^h$ | $n_e$ |
|---|---|---|---|
| 3 | 0.3, 0.5, 0.7 | 10158.66 | 190 |
| 5 | 0.1, 0.3, 0.5, 0.7, 0.9 | 10165.32 | 276 |

Figure 11 shows the computed vibration modes and corresponding final meshes

for different numbers of multiple cracks. Figures 11 (a) and (b) depict the vibration mode components under three-crack damage, while Figures 11 (c) and (d) show the vibration mode components under five-crack damage. It can be observed that the

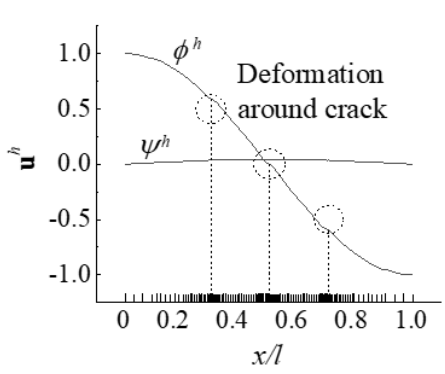


(a) Vibration mode $(\phi^h, \psi^h)$, $k = 1$, $n = 1$, $\alpha_1 = 0.3, \alpha_2 = 0.5, \alpha_3 = 0.7$

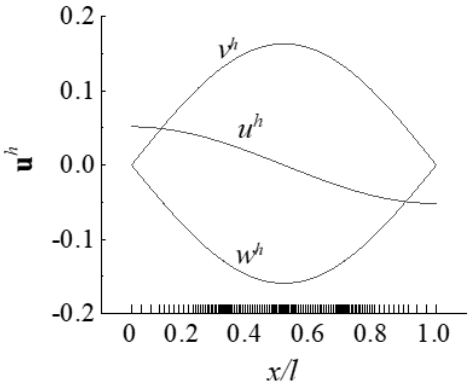


(b) Vibration mode $(u^h, v^h, w^h)$, $k = 1$, $n = 1$, $\alpha_1 = 0.3, \alpha_2 = 0.5, \alpha_3 = 0.7$

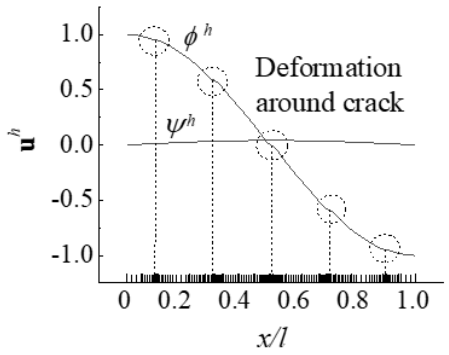


(c) Vibration mode $(\phi^h, \psi^h)$, $k = 1$, $n = 1$,
$\alpha_1 = 0.1, \alpha_2 = 0.3, \alpha_3 = 0.5,$
$\alpha_4 = 0.7, \alpha_5 = 0.9$

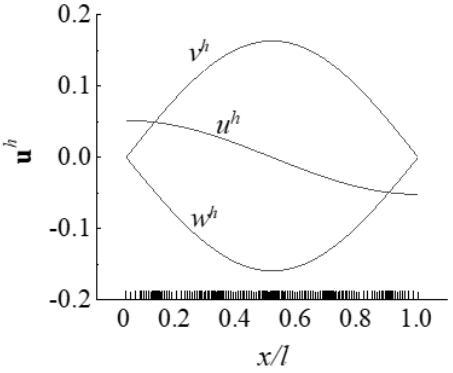


(d) Vibration mode $(u^h, v^h, w^h)$, $k = 1$, $n = 1$, $\alpha_1 = 0.1, \alpha_2 = 0.3, \alpha_3 = 0.5,$
$\alpha_4 = 0.7, \alpha_5 = 0.9$

**Figure 11.** Example 5: computed vibration modes and corresponding final meshes for different numbers of multiple cracks.

number and location of multiple-crack damage cause a corresponding disturbance to the vibration mode components, and the local subdivision and refinement domains of the meh changes with the change in the vibration mode location of the crack damage disturbance. The existence of multiple-crack damage causes multiple disturbances in the vibration modes of the shell, and hence more local domains need to be subdivided

and densified, resulting in a large number of elements in the global domain. These results show the reliability of the adaptive mesh refinement method in this study to the changes in mode shapes and modes under simultaneous multiple-crack damage.

## 7. Conclusions

In this study, an adaptive mesh refinement analysis of the finite element method for free vibration disturbance of moderately thick circular cylindrical shells with circumferential crack damage is implemented to derive the frequency solutions under variable circumferential wave numbers and discuss the free vibration disturbance by factors of crack damage, such as the location, depth, and number of cracks. The conclusions of this study can be summarised as follows.

(1) An adaptive finite element method and crack damage characterisation method for moderately thick circular cylindrical shells are proposed. By introducing the inverse power iteration method, error estimation, and mesh subdivision refinement technique for the analysis of finite element eigenvalue problems, an adaptive computation scheme is constructed for the free vibration problem of moderately thick circular cylindrical shells with circumferential crack damage.

(2) Typical numerical examples of benchmarks and frequency solutions of cracked shells under variable circumferential wave numbers confirmed that the established adaptive finite element solution for the free vibration of moderately thick circular cylindrical shells is suitable for solving the high-precision free vibration frequency and mode of cylindrical shell structures. The reliability, accuracy, and effectiveness of the proposed method and models were verified.

(3) The adaptive mesh refinement algorithm has good applicability for the analysis of cracked shells. The vibration mode was disturbed near the crack damage. In this study, the non-uniform mesh was adaptively optimised, and a relatively dense mesh was used near the crack to adapt to the change in vibration mode caused by crack damage.

(4) The occurrence of crack damage reduces the frequency of each order, and the greater the damage depth is, the greater the reduction degree. The crack damage generates the greatest disturbance to the rotational displacement, and the greater the damage degree is, the greater the disturbance amplitude. The number and location of cracks simultaneously affect the frequency value. An increase in the

number of cracks tends to increase the frequency as a whole. However, because the change in crack location will also reduce the frequency value in some order frequencies, the vibration modes near each crack damage will be disturbed. Compared with the uniform distribution, the frequency value of the concentrated distribution on one side of the crack has a higher value at low order and a lower value at high order. The vibration modes were disturbed near the uniformly distributed and centrally distributed crack damage. The different distribution forms of the same number of cracks have become an important factor affecting the vibration characteristics.

This study can be used as a reference for the adaptive finite element solution of free vibration of moderately thick circular cylindrical shells with cracks and it lays a foundation for further development of a high-performance computation method suitable for dynamic disturbance and damage identification analysis of general cracked structures. Furthermore, the error estimation and element refinement techniques of the finite element method have the potential to be extended in the future to the refined numerical model and high-precision computation field of general structural eigenvalue problems (displacement field) and solid stress (displacement derivative field).

## References

Ainsworth, M., Oden, J.T. (1992), “A procedure for a posteriori error estimation for h-p finite element methods”, *Computer Methods in Applied Mechanics and Engineering*, Vol. 101, pp. 73–96.

Ainsworth, M., Oden, J.T. (1993), “A unified approach to a posteriori error estimation using element residual methods”, *Numerische Mathematik*, Vol. 65, pp. 23–50.

Arbelo, M.A., SFMD Almeida, Donadon, M.V., Rett, S.R., Degenhardt, R., Castro, S., Kalnins, K. Ozolinset, O. (2014) “Vibration correlation technique for the estimation of real boundary conditions and buckling load of unstiffened plates and cylindrical shells” *Thin-Walled Structures*, Vol. 79 No. 1, pp. 119–128.

Arndt, M., Machado, R.D., Scremin, A. (2010), “An adaptive generalized finite element method applied to free vibration analysis of straight bars and trusses”, *Journal of Sound and Vibration*, Vol. 329 No.6, pp. 659–672.

Arthurs, C.J., Bishop, M.J., Kay, D. (2013), "Efficient simulation of cardiac electrical propagation using high-order finite elements II: adaptive p-version", *Journal of Computational Physics*, Vol. 253, pp. 443–470.

Aydin, K. (2013), "Free vibration of functionally graded beams with arbitrary number of surface cracks", *European Journal of Mechanics*, Vol. 42 No. 42, pp. 112-124.

Babuska, I, Rheinboldt, W.C. (1979), "Adaptive approaches and reliability estimates in finite element analysis", *Computer Methods in Applied Mechanics and Engineering*, Vol. 17 No. 3, pp. 519–540.

Babuska, I., Rheinboldt, W.C. (1978), "A-posteriori error estimates for the finite element method", *International Journal for Numerical Methods in Engineering*, Vol. 12, pp. 1597–1615.

Bao, G., Hu, G., Liu, D. (2012), "An *h*-adaptive finite element solver for the calculations of the electronic structures", *Journal of Computational Physics*, Vol. 231 No. 14, pp. 4967–4979.

Bespalov, A., Haberl, A., Praetorius, D. (2017), "Adaptive FEM with coarse initial mesh guarantees optimal convergence rates for compactly perturbed elliptic problems", *Computer Methods in Applied Mechanics and Engineering*, Vol. 317, pp. 318–340.

Chen, J.S. , Zhang, Y. (2006), "The analysis of the limit element method on the free vibration of the cylinder shell", *Machinery Design & Manufacture,* No. 11, pp. 16–17

Chen, X.D., Ye, K.S. (2016), "Analysis of free vibration of moderately thick circular cylindrical shells using the dynamic stiffness method", *Journal of Vibration and Shock,* Vol. 35 No. 6, pp. 84–90

Chestler, S.R., Creager, K.C. (2017), "Evidence for a scale-limited low-frequency earthquake source process", *Journal of Geophysical Research: Solid Earth*, Vol. 122 No. 4, pp. 3099-3114.

Dehghani, O.S., Esmaeilpour, E.H. and Vafaei, A.H. (2008), "Free vibration of cracked cylindrical shells"

Dey, T., Ramachandra, L.S. (2017), "Non-linear vibration analysis of laminated

composite circular cylindrical shells", *Composite Structures,* Vol. 163 No. 8.

Dong, W., Liu, Y., Xiang, Z. (2012), "An analytical method for free vibration analysis of functionally graded beams with edge cracks" *Journal of Sound & Vibration*, Vol. 331 No. 7, pp. 1686-1700.

Flugge (1973), Stresses in shells. Springer.

Gomez-Revuelto, I., Garcia-Castillo, L.E., Llorente-Romano, S., Demkowicz, L.F. (2012), "A three-dimensional self-adaptive *hp* finite element method for the characterization of waveguide discontinuities", *Computer Methods in Applied Mechanics and Engineering*, Vol. 249, pp. 62–74.

Greenberg, L. (1991), "A prüfer method for calculating eigenvalues of self-adjiont systems of ordinary differential equations: parts 1 and 2", Technical Report. TR91-24, University of Maryland at College Park, MD.

Grigorenko, A.Y., Puzyrev, S.V., Prigoda, A.P. and Khorishko, V. V. (2011), "Theoretical-experimental investigation of frequencies of free vibrations of circular cylindrical shells" *Journal of Mathematical Sciences*, Vol. 174 No. 2, pp. 254–267.

Grigorenko, Ya., A., Efimova, T.L., and Sokolova, L.V. (2010), "On one approach to studying free vibrations of cylindrical shells of variable thickness in the circumferential direction within a refined statement" *Journal of Mathematical Sciences*, Vol. 171 No. 4, pp. 548–563.

Hosseini-Hashemi, S., Fadaee, M. (2011), "On the free vibration of moderately thick spherical shell panel—a new exact closed-form procedure" *Journal of Sound and Vibration*, Vol. 330 No. 17, pp. 4352-4367.

Ide, S., Yabe, S., Tanaka, Y. (2016), "Earthquake potential revealed by tidal influence on earthquake size–frequency statistics", *Nature Geoscience*, Vol. 9 No. 11, pp. 834-837.

Jaan, Lellep, Larissa and Roots. (2010), "Vibrations of cylindrical shells with circumferential cracks", *Wseas Transactions on Mathematics*, Vol. 9 No. 9, pp. 689-699.

Jafari, A.A., Bagheri, M. (2006), "Free vibration of non-uniformly ring stiffened

cylindrical shells using analytical, experimental and numerical methods", *Thin-Walled Structures*, Vol. 44 No. 1, pp. 82-90.

Jin, C.C., Zhu, x., Li, T. and Fang, M. (2018), "Coupled vibration feature analysis for a fluid-filled cylindrical shell with a circumferential surface crack", *Journal of Vibration and Shock*, Vol. 37 No. 23 pp. 71-77.

Kang, B., Riedel, C.H. and Tan, C.A. (2003), "Free vibration analysis of planar curved beams by wave propagation", *Journal of Sound and Vibration*, Vol. 260 No. 1, pp. 19–44.

Kurochkin, S.V. (2014), "Indexing of eigenvalues of boundary value problems for Hamiltonian systems of ordinary differential equations", *Computational Mathematics and Mathematical Physics*, Vol. 54 No. 3, pp. 439–442.

Lee, H.W., Kwak, M.K. (2015), "Free vibration analysis of a circular cylindrical shell using the rayleigh–ritz method and comparison of different shell theories" *Journal of Sound and Vibration*, Vol. 353, pp. 344-377.

Li, Q.S., (2001), "Free vibration analysis of non-uniform beams with an arbitrary number of cracks and concentrated masses", *Journal of Sound and Vibration*, Vol. 252 No. 3, pp. 509–525.

Love A. E. H. (2013), "A treatise on the mathematical theory of elasticity" Cambridge University Press, Cambridge.

Pellicano, F. (2007), "Vibrations of circular cylindrical shells: theory and experiments" *Journal of Sound & Vibration*, Vol. 303 Nos. 1-2, pp. 154–170.

Qu, Y., Hua, H., Meng, G. (2013), "A domain decomposition approach for vibration analysis of isotropic and composite cylindrical shells with arbitrary boundaries", *Composite Structures*. Vol. 95, pp. 307–321.

Roots, L. (2014), "Non-axisymmetric Vibrations of Stepped Cylindrical Shells Containing Cracks", 2014 International Conference on the Mechanics of Biological Systems and Materials, Seoul.

Schillinger, D., Rank, E. (2011), "An unfitted hp-adaptive finite element method based on hierarchical B-splines for interface problems of complex geometry", *Computer Methods in Applied Mechanics and Engineering*, Vol.

200 Nos. 47–48, pp. 3358–3380.

Sivadas, K. R., Ganesan, N. (1994), "Free vibration and material damping analysis of moderately thick circular cylindrical shells", *Journal of Sound & Vibration*, Vol. 172 No. 1, pp. 47-61.

Wang, X.H., Redekop, D. (2011), "Natural frequencies analysis of moderately-thick and thick toroidal shells". *Procedia Engineering*, Vol. 14 No. 2259, pp. 636-640.

Wang, Y. (2021), Adaptive analysis of damage and fracture in rock with multiphysical fields coupling, Springer Press.

Wang, Y.L. (2020a), "Adaptive finite element–discrete element analysis for striatal movement and microseismic behaviors induced by multistage propagation of three-dimensional multiple hydraulic fractures", *Engineering Computations*, Vol. 38 No. 5, pp. 1350–1371.

Wang, Y.L. (2020b), "An h-version adaptive FEM for eigenproblems in system of second order ODEs: vector Sturm-Liouville problems and free vibration of curved beams", *Engineering Computations*, Vol. 37 No. 1, pp. 1210–1225.

Wang, Y.L., Ju, Y., Chen J.L., Song J.X. (2019), "Adaptive finite element–discrete element analysis for the multistage supercritical $CO_2$ fracturing of horizontal wells in tight reservoirs considering pre-existing fractures and thermal-hydro-mechanical coupling", *Journal of Natural Gas Science and Engineering*, Vol. 61, pp. 251–269.

Wang, Y.L., Ju, Y., Yang, Y.M. (2018a), "Adaptive finite element–discrete element analysis for microseismic modelling of hydraulic fracture propagation of perforation in horizontal well considering pre-existing fractures", *Shock and Vibration*, pp. 1–14.

Wang, Y.L., Ju, Y., Zhuang, Z., Li, C.F. (2018b), "Adaptive finite element analysis for damage detection of non–uniform Euler–Bernoulli beams with multiple cracks based on natural frequencies", *Engineering Computations*, Vol. 35 No. 3, pp. 1203–1229.

Wang, Z.Q., Huang, L.H., Li, X.B. (2017), "Vibration analysis of circular cylindrical shells under arbitrary boundary conditions", *Ship Science and Technology,* Vol.

39 No. 4, pp. 24–29

Wei, Y., Xiao, K.Y., Tong, Y.K. (2014), "Summary for ultimate bearing capacity research methods of engineering-structure containing flaws" Shanxi Architecture.

Weingarten, V.I. (2012), "Free Vibration of Thin Cylindrical Shells", *Aiaa Journal*, Vol. 2 No. 4, pp. 32.

Wiberg, N.E, Bausys, R., Hager, P. (1999a), "Improved eigenfrequencies and eigenmodes in free vibration analysis", *Computers and Structures*, Vol. 73 Nos. 1–5, pp. 79–89.

Wiberg, N.E., Bausys, R., Hager, P. (1999b), "Adaptive *h*-version eigenfrequency analysis", *Computers and Structures*, Vol. 71 No. 5, pp. 565–584.

Wilkinson, J.H, Reinsch, C. (1971), "Linear algebra, handbook for automatic computation", Springer-Verlag, New York.

Wilkinson, J.H. (1965), "The Algebraic Eigenvalue Problem", Clarendon Press, Oxford.

Yin, T., Lam, Heung-Fai. (2013), "Dynamic analysis of finite-length circular cylindrical shells with a circumferential surface crack" *Journal of Engineering Mechanics*, Vol. 139 No. 10, pp. 1419-1434.

Yin, T., Li, Q.S., Zhu, H.P., (2013), "A new solution method for vibration analysis of circular cylindrical thin shells with a circumferential surface crack." *Advanced Materials Research* Vol. 639-640 No. 1, pp. 1003–1009.

Yoon, H.I., Son, I.S., Ahn, S.J. (2007), "Free vibration analysis of Euler-Bernoulli beam with double cracks", *Journal of Mechanical Science and Technology,* Vol. 21, pp. 476–485.

Zheng, S., Yu, Y., Qiu, M., Wang, L., Tan, D. (2021), "A modal analysis of vibration response of a cracked fluid-filled cylindrical shell" *Applied Mathematical Modelling*, Vol. 91, pp. 934-958.

Zhu, X., Li, T. Y., Zhao, Y., Yan, J. (2007), "Vibrational power flow analysis of thin cylindrical shell with a circumferential surface crack" *Journal of Sound & Vibration*, Vol. 302 Nos. 1-2, pp. 323-349.

Zienkiewicz, O.C, Zhu, J.Z. (1992), "The superconvergent patch recovery (SPR) and

adaptive finite element refinement", *Computer Methods in Applied Mechanics and Engineering*, Vol. 101 Nos. 1–3, pp. 207–224.

Zienkiewicz, O.C. (2006), "The background of error estimation and adaptivity in finite element computations", *Computer Methods in Applied Mechanics and Engineering*, Vol. 195 Nos. 4–6, pp. 207–213.

Zienkiewicz, O.C., Taylor, R.L. and Zhu, J. (2015), "The finite element method: its basis and fundamentals (7th Edition)", Oxford, UK: Elsevier (Singapore) Pte Ltd.